SYNERGIES BETWEEN X-BAND FOR LINEAR COLLIDERS AND LIGHT SOURCES

M. Dehler, J.-Y. Raguin, A. Citterio, A. Falone, PSI, Villigen PSI, Switzerland
W. Wuensch, G. Riddone, A. Grudiev, R. Zennaro, CERN, Geneva, Switzerland

Abstract

To compensate nonlinearities in the longitudinal phase space at the injector prototype of the PSI-XFEL, PSI requires a high frequency RF structure in X band. At the same time CLIC is pursuing a program for producing and testing high gradient RF structures in the X band, exploring the effect of different geometries and materials on break down limits and rates. This makes it interesting to share work and expense in designing and producing a common CLIC/PSI-XFEL structure. It would provide new data for the CLIC break down tests and at the same time be a safe and low risk solution for the more relaxed operating gradient used at the PSI-XFEL. In addition the prolonged operation of such a structure in the PSI FEL injector, albeit not at CLIC parameters, constitutes a good quality test for the manufacturing procedures employed.

INTRODUCTION

Within the context of the JLC-X and NLC projects, a considerable effort has been going on in developing high power X band RF systems for high energy e^+e^- colliders[1]. After the conclusion of these projects, the recent decision by CLIC to change their principal RF frequency from 30 GHz to a European X band frequency near 12 GHz has given a renewed push to X band development. A big RF structure fabrication and testing program involving major laboratories around the world is under way, R&D efforts have been directed in adapting standard RF equipment, from high power klystrons to splitter and loads, to the new frequency.

Interestingly, X band technology is slowly leaking into other applications. The LCLS FEL uses a X band structure to compensate nonlinearities in the longitudinal phase space in order to improve bunch compression. The European FEL projects SPARC, FERMI@ELETTRA and PSI-XFEL also plan to employ X band RF for the same purpose. There is also a discussion going on to use X band for compact medical accelerators[2].

Where the SPARC project is staying with RF structures at the NLC/JLC frequency of 11.424 GHz, PSI has decided to follow the new European standard at 11.992 GHz. That way, an optional future operation of the PSI-XFEL in a few bunch or multi bunch operation mode is still possible (given that the current setup uses already European S/L band). Int that context, a klystron is currently under development by SLAC, an adapted version of type XL4 to be baptized XL5. The X band structure is being developed within a collaboration between PSI and CERN, optimizing synergy on both sides. The structure has several purposes, being submitted to break down tests at CERN, being used in the PSI-XFEL, which is, despite different operating parameters, an ultra long performance test quite important for CLIC.

At the PSI-XFEL, we have only limited power, in the order of 40 MW at the structure after taking account of waveguide losses, and need to generate beam voltages up to 30 MeV, which requires a fairly efficient structure. On the other hand, the beam passing through has a relatively modest energy of 250 MeV, so that we are relatively sensitive to transverse wakes. So the structure needs to make a good compromise between a high shunt impedance, generally associated with low apertures, and a low transverse kick, demanding the opposite.

As a generic type, we use a structure with a $5\pi/6$ phase advance and an active length of 750 mm similar to NLC type H75. Since the structure should not be used to test higher order mode damping, it will not have any HOM dampers. On the other hand, two wake field monitors near the beginning and the end of the structure are foreseen, which will help to align the structure to the beam and to minimize transverse kicks. Wakefield monitors are also planned for CLIC structures and their implementation in the PSI-FEL structures will represent an important performance test.

FUNDAMENTAL MODE PROPERTIES

In terms of simplicity and cost a single structure with 750 millimeter active length is the most appropriate solution for the PSI-XFEL requirements. The NLC structure type H75 ($5\pi/6$ phase advance) has been chosen as the most suitable candidate for the testing program. The original H75 design, optimized for iris aperture, thickness and ellipticity of the iris varying along the structure, provides an accelerating gradient of 65 MV/m for 80 MW input power and was successfully tested up to 100 MV/m with a SLAC mode launcher [3]. The relevant parameters of the adopted X-band cavity are summarized in Table1.

The constraints related to the beam dynamics requirements for the linearization of the longitudinal phase space fix the deceleration of the beam to 30 MeV. The gradient is maintained constant along the structure: Fig. 1 shows that, over 72 cells, the average gradient is 40 MV/m – the required input power to achieve such gradient is a modest 29 MW.

Because of the constant gradient design choice, the iris diameter changes along the structure, the lower limit be-

Table 1: Specifications

parameter	value
Beam Voltage	30 MeV
Max. Power	29 MW
Iris diameter	9.1 mm (avg.)
Wake field monitors	up/downstream
Operating temp.	40 deg. C
Fill time	100 ns
Repetition rate	100 Hz

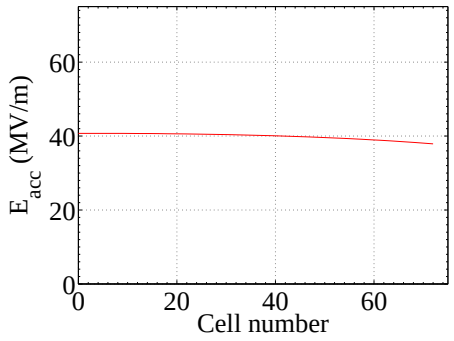

Figure 1: Decelerating gradient along the structure.

ing fixed by the deleterious effects of the short-range wake fields. As can be seen in Fig. 2, the iris diameter changes linearly with the number of cells: the mean aperture at 9.1 millimeter makes it a relatively open structure.

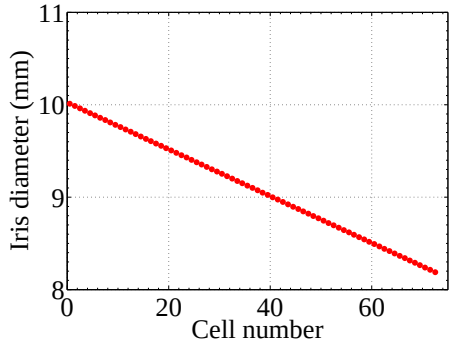

Figure 2: Variation of the iris aperture along the structure. The first cell has 9.986 mm iris diameter, the last one 8.239 mm.

The large phase advance of $5\pi/6$ offers two main advantages: The first, it means an intrinsically lower group velocity even at large apertures, providing a relatively high gradient and moderate required input power, and the second, smaller transverse wakes, since a longer cell means a smaller number of irises per structure. The variation of the group velocity and of the r/Q along the structure are shown in Fig. 3 and Fig. 4 respectively.

Concerning the velocity group variation, the v_g/c is 3.7% at the level of the first regular cell and decreases to 1.6% at

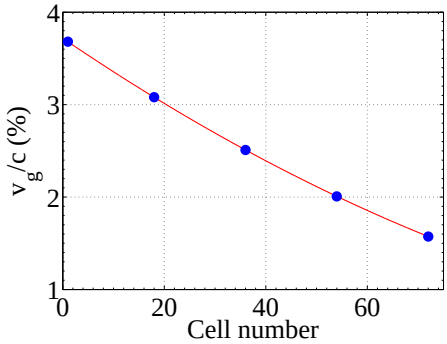

Figure 3: Variation of the group velocity along the structure.

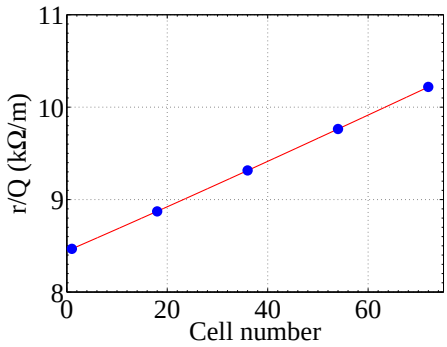

Figure 4: Variation of the r/Q along the structure.

the last regular cell. The r/Q value increases quasi linearly from 8.5 kΩ/m to 10.2 kΩ/m and the average Q-value computed is about 7150. The filling time of the structure is about 100 ns.

The input and output coupler design is based on the SLAC mode launcher design ([3]), which converts a rectangular TE_{01} waveguide mode into the circular TM_{01} waveguide mode of the X-band structure. The big advantage of this design is the reduced surface field, due to the rounded and thickened iris horns and the coupling the power through the broad wall of the feed waveguide. The dimensions of the cells between the mode launcher and the structure ends are used to optimize the matching, as can be seen in Fig. 5 and Fig. 6.

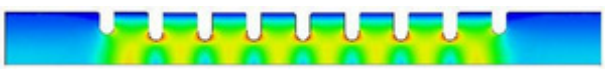

Figure 5: Electric field profile showing the good matching into upstream cells.

WAKE FIELD MONITOR

To measure the beam offset inside the structure, we want to couple to the lowest dipole mode. A minimum perturbation of the fundamental mode and maximum information

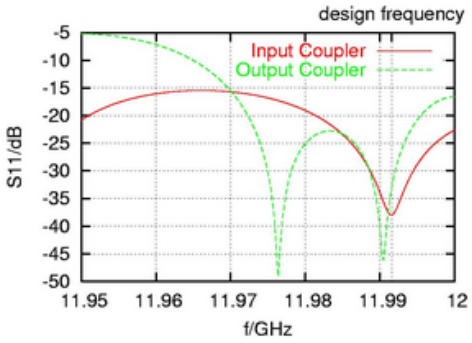

Figure 6: Reflexion coefficient for the input and output matching cells.

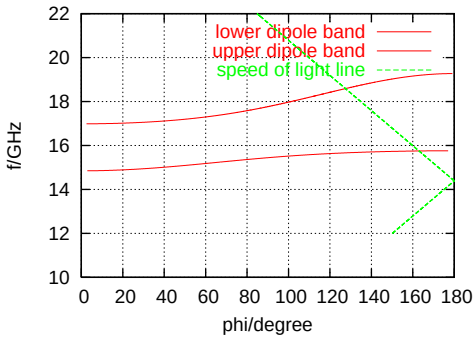

Figure 7: Dispersion diagram of lowest two dipole bands in cell 36.

in the output signal, together with an easy post processing, are the principal design criteria. Where and how to couple, what to expect from the measurement is explained in the following.

Location

We start by looking at the dispersion of the lowest dipole bands of a typical cell, shown in figure 7. As in a classical $2\pi/3$ structure we have hybrid HEM type dipole modes; the lower dipole band starts at zero phase with a strong TE type characteristic morphing into a TM characteristic as the phase approaches 180 degrees. At $5\pi/6$, the cell is longer, so the speed of light line and the dispersion curve are crossing at opposite slopes (This holds for all cells in the design), so the beam will excite a backward wave in the lowest dipole band. The synchronous phase is relatively near to 180 degrees.

The distribution of bandwidths and synchronous frequencies of the lowest dipole band inside the whole structure is shown in figure 8. From this, we can identify three different frequency regions. Dipole modes with resonances in the region of 15.3 to 16.1 GHz will be trapped modes, which are localized in only part of the structure, since cells at the beginning and the end can not propagate these frequencies. These trapped modes start in one of the upstream cells with a field distribution corresponding to a π mode and continue with a decreasing phase advance to

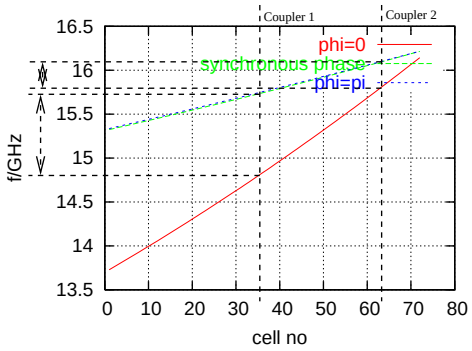

Figure 8: Limits of lowest dipole band and synchronous frequency versus cell number. Also shown the location of the wake field couplers with their respective bandwidths.

the downstream cell, where it goes to zero. The excitation by the beam is most pronounced in the cell, where the resonance corresponds to the synchronous frequency and phase, which is close to 180 degrees. Modes with frequencies below 15.3 GHz (the π mode of cell 1) will extend from the input coupler to the cell where the phase advance goes to zero. Most of these modes will have only a weak kick factor, since their frequency does not correspond to one of the synchronous frequencies. The last region contains modes above 16.1 GHz, the modes extend into the output coupler and have a high kick.

With this in mind, we are able to choose suitable locations for the wake field monitors. We assume that the wake field monitor will couple only weakly to the resonant fields and will not distort the modal pattern inside the structure. Dipole wakes excited by offsets in the upstream half of the structure will correspond to modes which are concentrated in the middle of it. Actually, if we put a monitor in cell 36, it will have a bandwidth of 14.8 to 15.7 GHz (the width of the dipole band in cell 36), the corresponding modes have their synchronous phases in the upstream half and will signal offsets there. For the downstream coupler, we are restricted of the dipole band there – a reasonable compromise is putting it in cell 63, which receives wakes excited in cells 40-63.

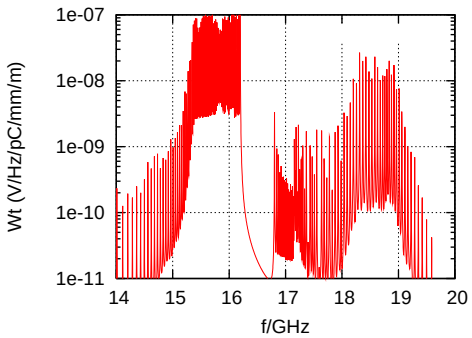

Figure 9: Transverse wake impedance for the structure as calculated via the dual resonator model[4].

Wake monitor signals and wakes, to be shown in the following, were obtained from a dual resonator equivalent circuit, where the elements of the resonators describing the TE and TM components of the hybrid dipole mode and their mutual couplings are fitted from the results of numerical computations This method is described in more detail in [4], and gives valid results for the two lowest dipole bands. The transverse impedance computed for the whole 72 cell structure is shown in figure 9. As can be expected from the distribution of frequencies shown in figure 8, modes below 15.3 GHz contribute only weakly to the overall wake, only in the region from 15.3 to 16.2 GHz we see a strong coupling to the beam.

Monitor Design

What are the criteria for the pickup measuring the transverse wakes? In order to effectively measure the position, the wake monitor should reject signals coming from the fundamental mode power as well as longitudinal higher order modes, which are all transverse magnetic fields. This type of field can best be rejected by selectively coupling to the transverse electric components of the hybrid dipole modes, something, which is obtained by a suitable orientation of the coupling waveguide.

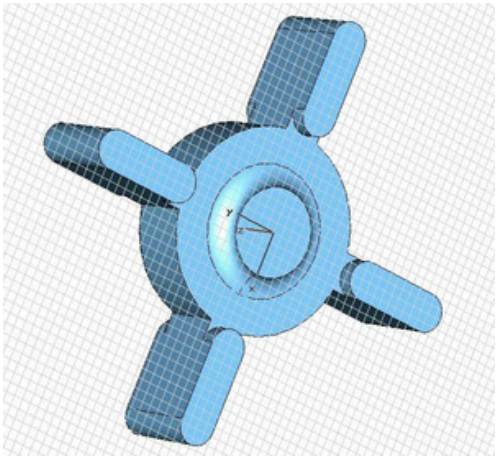

Figure 10: Wake monitor cell 36 – side coupled output waveguide with electric shorted on one side.

One option is to realize it using radially oriented waveguides coupling head on to the cavity cell and a second having a waveguide in parallel to the beam axis being side coupled – similar to the design of the damped detuned structure, but coupling only to one select cell. The side coupled version has the advantage, that we can have a longer wave guide damping down any residual signal from the fundamental mode, which may enter due to finite mechanical tolerances. That way, there is also enough space to integrate a transition from the waveguide to coaxial and use a standard 50 Ω vacuum feed through to connect the measurement front end. We went for this option, the coupler design chosen is similar to the HOM coupled cells of the damped detuned structures, the difference being that we couple only to one cell and have the wave guide electrically shorted on one side as shown in figure 10.

The coupling strength corresponds to a loaded Q in the order of 800 at a phase advance of zero (where the modal patterns couples best) and gives a sufficient signal strength. The effect on the fundamental mode parameters is only minor – a 10 % drop in group velocity and in Q factor, R/Q stays virtually unchanged.

Signals

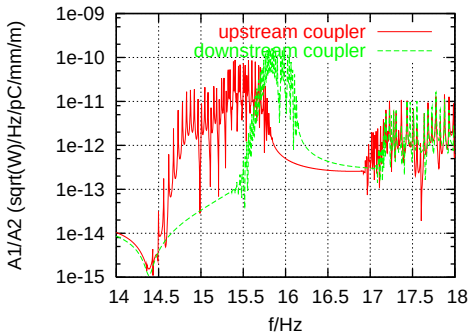

Figure 11: Output signals from up- and downstream monitors vs. frequency.

Figure 11 shows the signal spectra computed for the up- and downstream couplers. As can be expected from the previous discussion, we see two distinct frequency bands corresponding to the synchronous frequencies in the two parts of the structure.

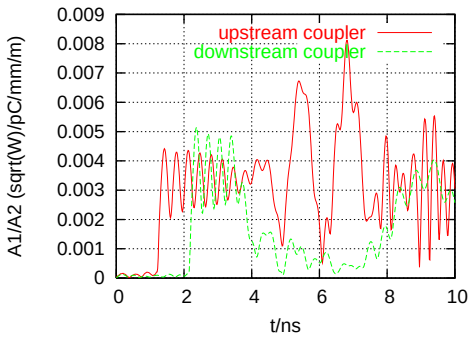

Figure 12: Signal envelope from up- and downstream monitors vs. time.

Before we look at other properties of these monitors, we should explain a little more in details, what is going on inside the structure. A dipole mode is excited by the beam dominantly in the 'synchronous' cells, where his resonant frequency corresponds to the synchronous one. The mode does not build up instantaneously, but the energy deposited by the beam in this synchronous cell needs time to get distributed in the structure – the distance between the synchronous cell and the wake field monitor leads to a time delay, before the signal shows up in the monitor signal.

Signals from different part of the structure have a different delay. In the time domain (figure 12), this shows up as an initial rectangular pulse (with some beating on top) of 2-3 nanoseconds length.

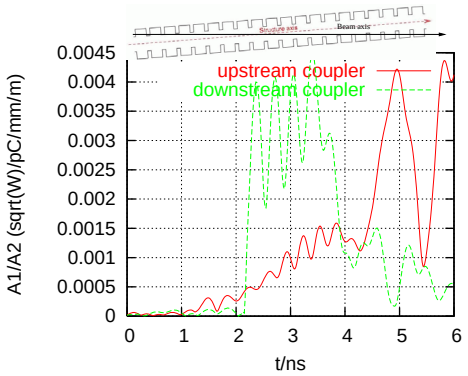

Figure 13: Signal envelope up- and downstream monitors vs. time assuming structure axis tilted to beam axis.

The beam offset in individual parts of the structure is correlated to different synchronous frequencies and this in turn with different delays in the time domain signal. So it is a valid question, whether it is possible to identify also tilts with respect to the beam. In this case, the middle of the structure is aligned with the beam axis, whereas the extremities would be offset generating a transverse signal. The resultant wake monitor signals are shown in figure 13. The upstream monitor is the more significant one in this case, since it sees the total front half of the structure. Where a constant offset gives a more or less rectangular pulse like in fig. 12, we see now a ramp, starting at zero (no offset in the middle) and growing linearly to the peak (high offset at beginning). The downstream signal shows a similar slope, which is not as pronounced, since it sees only part of the structure.

We simulated also the effect of a bend in the structure, but here dispersion effects smearing out the signal are too strong to obtain a clear pattern in the output signal.

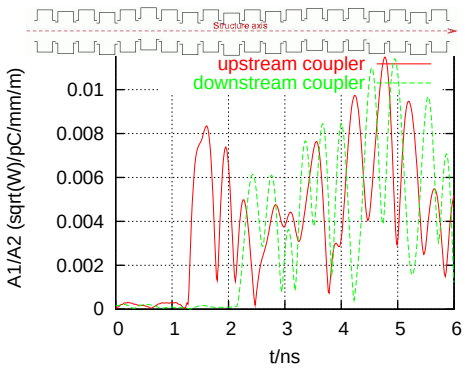

Figure 14: Signal envelope up- and downstream monitors vs. time assuming random, uncorrelated misalignment of individual cells in the structure.

A last important topic is the resolution of the monitors. Apart from the usual suspects – thermal noise in pickup and front end and spurious signals from other sources – we have a significant contribution from the random non correlated misalignment of individual cells. As the beam passes through the structure seeing these random offsets, it will, independent of the offset, excite wake fields and wake signals, which we will see as a noisy background to the measurement. To estimate this contribution, we implemented this feature into the equivalent circuit model to simulate it. Figure 14 shows an example for the output signal. Comparing the peak random offset signal in the first four nanoseconds, roughly 8 mV/pC/mm/m, by that of a constant offset signal (fig. 12), 4 mV/pC/mm/m, gives the impact on the measurement. Or said otherwise, a structure with a random cell offset of 1 μm rms will create a signal proportional to a systematic offset of 2 μm – the wake monitors will have a resolution limit of 2 μm. Given, that we would like to see resolutions below 10 μm, corresponding to a mechanical cell to cell alignment of better than 5 μm, which seems entirely feasible.

CONCLUSION AND OUTLOOK

A new design X band structure for the new CLIC reference frequency has been presented, to be used for high gradient testing at CLIC and as a prototype structure for the PSI-XFEL injector. It offers an efficient fundamental mode performance with a wide aperture minimizing transverse wake field effects. The wake field monitors included in the design will allow a very high quality alignment to the beam giving information about offsets and tilts of the structure.

With the RF design finished, we are currently in the transition to the mechanical design, which will be followed by manufacturing and low level RF tests. Structures for high power testing are expected to be ready in autumn 2009.

REFERENCES

[1] C.E. Adolphsen et al, " International study group progress report on linear collider development", SLAC-R-559, SLAC-R-0559, SLAC-559, SLAC-0559, KEK-REPORT-2000-7, LCC-0042, Apr 2000. 286pp. ISG Progress Report, April 2000.

[2] R. Zennaro, "Linacs for Hadrontherapy: CABOTO, a X-band CArbon BOoster for Therapy in Oncology". proc. X-Band RF Structure and Beam Dynamics Workshop - 44th ICFA Advanced Beam Dynamics Workshop, Nov 30 - Dec 04 2008, Daresbury UK, to be published.

[3] C. Nantista, S. Tantami and V. Dolgashev, "Low-field accelerator structure couplers and design techniques", Phys. Rev. Special Topics - Accelerators and Beams, Vol. 7, 072001 (2004).

[4] R.M. Jones, C.E. Adolphsen, J.W. Wang, Z. Li, "Wakefield damping in a pair of X-band accelerators for linear colliders", Phys.Rev.ST Accel.Beams 9:102001,2006.